

EFFECT OF THERMO DIFFUSION AND CHEMICAL REACTION ON NON DARCY
CONVECTIVE HEAT AND MASS TRANSFER FLOW
IN A VERTICAL CHANNEL WITH RADIATION

Dr. Y. Madhusudhana Reddy^{1*} & Prof. D. R. V. Prasada Rao²

¹Associative Professor, Dept. of Mathematics,
¹Sri venkateswara Institute of Technology, Anantapur, Andhrapradesh, India
E-mail: ymsmadhu@gmail.com

²Professor, Dept of Mathematics, S. K. University, Anantapur, Andhrapradesh, India
E-mail: drv_atp@yahoo.in

(Received on: 05-04-12; Accepted on: 25-04-12)

ABSTRACT

We discuss the effect of radiation, diffusion and chemical reaction on the mixed convective heat and mass transfer flow of a viscous electrically conducting fluid through a porous medium in a vertical channel in the presence of heat generating sources. By employing a regular perturbation technique with a porous parameter δ acting on the flow phenomena is analyzed graphically. The rate of heat and mass transfer are evaluated numerically.

Key Words: Thermo diffusion, Chemical reaction, Non darcy, Vertical Channel, Radiation, Porous medium.

1. INTRODUCTION

Heat transfer in the case of homogeneous fluid saturated porous medium has been studied with relation to different applications like dynamics of hot underground springs, terrestrial heat flow through aquifers, hot fluid and ignition from displacements in reservoir engineering, heat exchange between soil and atmosphere, flow of moisture through porous industrial materials and heat exchange with fluidized beds. Mass transfer in isothermal conditions has been studied with applications to problems of mixing of fresh and salt water in aquifers, miscible displacements in oil reservoirs, spreading of solutes in fluidized beds and crystal washers, salt leaching in soils etc. Prevention of salt dissolution into lake waters near the sea shores has become a serious problem for research.

Coupled heat and mass transfer phenomenon in porous media is gaining attention due to its interesting applications. The flow phenomenon is relatively complex rather than that of the pure thermal convection process. Underground spreading chemical wastes and other pollutants, grain storage, evaporation cooling and solidification are the few other application areas where the combined thermo-solutal natural convection in porous media are observed. Combined heat and mass transfer by free convection under boundary layer approximations has been studied by Bejan and Khair[2], Lai and Kulacki[4] and Murthy and Singh[5]. Coupled heat and mass transfer by mixed convection in Darcian fluid-saturated porous media has been analysed by Lai[3]. The free convection heat and mass transfer in a porous enclosure has been studied recently by Angirasa et al[1]. The combined effects of thermal and mass diffusion in channel flows has been studied in recent times by a few authors, notably Nelson and Wood[6,7], and others[11,12].

In almost all these works the boundary layer formulation of Darcy's law, the energy and diffusion equations were used. Non-Darcy effects on natural convection in porous media have received a great deal of attention in recent years because of the experiments conducted with several combinations of solids and fluids covering wide range of governing parameters which indicates that the experimental data for systems other than glass water at low Rayleigh numbers do not agree with theoretical predictions based on the Darcy flow model. This divergence in the heat transfer results has been reviewed in detail in the works Prasad et al [8] among others.

For some industrial applications such as glass production and furnace design in space technology applications, Cosmical flight aerodynamics, rocket propulsions systems, plasma physics which effects can be significant. Raptis and Perdikis[9] have studied the effects of thermal radiation and free convection flow past a moving vertical plate.

Corresponding author: Dr. Y. Madhusudhana Reddy^{1}, *E-mail: ymsmadhu@gmail.com

In many chemical engineering processes, there does occur the chemical reaction between a foreign mass and the fluid in which the plate is moving. These processes take place in numerous industrial applications viz., polymer production, manufacturing of ceramics or glassware and food processing.

In this paper we deal with the non-darcy effects on two-dimensional laminar simultaneous heat and mass transfer flow of a viscous, incompressible, electrically conducting and chemically reacting fluid through a porous medium confined in a vertical channel. The equations of continuity, linear momentum, energy and diffusion which govern the flow fields are solved by employing a regular perturbation technique. The behaviour of the velocity, temperature and concentration, skin friction, Nusselt number and Sherwood Number has been discussed for variations in the governing parameters.

2. FORMULATION OF THE PROBLEM

We consider a coupled heat and mass transfer flow of a viscous electrically conducting fluid through a porous medium confined in a vertical channel bounded by porous flat walls in the presence of heat generating sources, transverse magnetic field effects and a first order chemical reaction. The flow is assumed to be steady, laminar and two-dimensional and the surface is maintained at constant temperature and concentration, As the plates are sufficiently long, the flow variables does not depend on the vertical and axial co-ordinates. It is also assumed that the applied magnetic field is uniform and that magnetic Reynolds number is small so that the induced magnetic field is neglected. In addition, there is no applied electric field and all of the Hall effect, viscous dissipation and Joule heating are neglected. All thermophysical properties are constant except the density in the buoyancy terms of the linear momentum equation which is approximated according to the Boussinesq approximation, Under these assumptions, the equations describing the physical situation are given by

$$\frac{\partial v}{\partial y} = 0 \quad (2.1)$$

$$v \frac{\partial u}{\partial y} = \nu \frac{\partial^2 u}{\partial y^2} + \beta g (T - T_e) + \beta^* g (C - C_e) - \frac{\sigma B_0^2 u}{\rho} - \left(\frac{\nu}{k_1}\right)u - \frac{\delta F}{\sqrt{k}} u^2 \quad (2.2)$$

$$\rho_0 C_p v \frac{\partial T}{\partial y} = \lambda \frac{\partial T}{\partial y^2} + Q(T - T_e) - \frac{\partial(q_R)}{\partial y} \quad (2.3)$$

$$v \frac{\partial C}{\partial y} = D \frac{\partial C}{\partial y^2} - \gamma_1 C + K_{11} \frac{\partial^2 T}{\partial y^2} \quad (2.4)$$

where y is the horizontal or transverse coordinate, u is the axial velocity, v is the transverse velocity, T is the fluid temperature, C is the concentration, T_e is the ambient temperature, C_e is the ambient concentration and $\rho, g, \beta, \beta^*, \mu, \sigma, B_0, Q, D$ and γ_1 are the density, gravitational acceleration, coefficient of thermal expansion, coefficient of concentration expansion, dynamic viscosity, fluid electrical conductivity, magnetic induction, heat generation/absorption coefficient, mass diffusion coefficient, chemical reaction parameter and K_{11} is the cross diffusivity respectively. The physical boundary conditions for the problem are

$$\begin{aligned} u(-L) = 0, v(-L) = v_w, T(-L) = T_1, C(-L) = C_1 \\ u(+L) = 0, v(+L) = v_w, T(+L) = T_2, C(+L) = C_2 \end{aligned} \quad (2.5)$$

where $v_w > 0, T_1, T_2$ and C_1, C_2 are the suction velocity, surface temperature and concentration on $y = \pm L$ respectively. Invoking Rosseland approximation for radiative heat flux [9].

$$q_r = -\frac{4\sigma^*}{3\beta_R} \frac{\partial T'^4}{\partial y}$$

Expanding T'^4 in Taylor series about T_e and neglecting higher order terms we get

$$T'^4 \cong 4TT_e^3 - 3T_e^4$$

q_r represents the radiation heat flux in the y direction, σ^* the Stefan-Boltzman constant and β_R the mean absorption coefficient.

In order to write the governing equations and boundary conditions in the dimensionless form the following non-dimensional quantities are introduced

$$y' = \frac{y}{L}, u' = \frac{u}{(v/L)}, \theta = \frac{T - T_1}{T_2 - T_1}, C' = \frac{C - C_1}{C_2 - C_1}$$

the equations after dropping the dashes are

$$\frac{d^2 u}{dy^2} + S \frac{du}{dy} + G\delta(\theta + N C) - \delta(M^2 + D^{-1})u - (\delta^2 \Lambda)u^2$$

$$\frac{d^2 \theta}{dy^2} + SP_1 \frac{d\theta}{dy} - \alpha P_1 \theta = 0$$

$$\frac{d^2 C}{dy^2} + SSc \frac{dC}{dy} - k Sc C = -\frac{ScSo}{N} \frac{\partial^2 \theta}{\partial y^2}$$

where

$$P = \frac{\mu C_p}{\lambda} \quad (\text{Prandtl Number})$$

$$Sc = \frac{v}{D} \quad (\text{Schmidt Number})$$

$$k = \frac{\gamma_1 L^2}{v} \quad (\text{Chemical reaction parameter})$$

$$M^2 = \frac{\sigma B_0^2 L^2}{\rho_0 v} \quad (\text{Hartman Number})$$

$$N = \frac{\beta^* \Delta C}{\beta \Delta T} \quad (\text{Buoyancy ratio})$$

$$D^{-1} = \frac{L^2}{k_1} \quad (\text{Darcy parameter})$$

$$N_1 = \frac{\lambda \beta_R}{4\sigma^* T_e^3} \quad (\text{radiation parameter})$$

$$\alpha = \frac{QL^2}{\lambda} \quad (\text{Heat source parameter})$$

$$So = \frac{K_{11} \beta^*}{\gamma \beta} \quad (\text{soret parameter})$$

$$\Lambda = FD^{-1/2} \quad (\text{Inertia parameter or Foechhimer Number})$$

$$N_2 = \frac{3N_1}{3N_1 + 4}$$

$$P_1 = PN_2$$

The non-dimensional boundary conditions are

$$u(\pm 1) = 0, \theta(-1) = 0, C(-1) = 0$$

$$\theta(+1) = 1, C(+1) = 1$$

3. ANALYSIS OF THE FLOW

The governing equations of the flow, temperature and concentration are coupled non-linear differential equations. Assuming the porosity δ to be small, we write

$$u(y) = u_0(y) + \delta u_1(y) + \delta^2 u_2(y) + \dots \tag{3.1a}$$

$$\theta(y) = \theta_0(y) + \delta \theta_1(y) + \delta^2 \theta_2(y) + \dots \tag{3.1b}$$

$$C(y) = C_0(y) + \delta C_1(y) + \delta^2 C_2(y) + \dots \tag{3.1c}$$

Substituting the above expansions (3.1a)-(3.1c) in the equations (2.6)-(2.8) and equating the like powers of δ , we obtain equations to the zeroth order as

$$\frac{d^2 u_0}{dy^2} + S \frac{du_0}{dy} = \pi \quad (3.2)$$

$$\frac{d^2 \theta_0}{dy^2} + SP \frac{d\theta_0}{dy} - \alpha P \theta_0 = 0 \quad (3.3)$$

$$\frac{d^2 C_0}{dy^2} + SSc \frac{dC_0}{dy} - \gamma C_0 = -\frac{ScSo}{N} \frac{\partial^2 \theta_0}{\partial y^2} \quad (3.4)$$

The first order equations are

$$\frac{d^2 u_1}{dy^2} + S \frac{du_1}{dy} = -G(\theta_0 + NC_0) + (D^{-1} + M^2)u_1 - Au_0^2 \quad (3.5)$$

$$\frac{d^2 \theta_1}{dy^2} + SP \frac{d\theta_1}{dy} - \alpha P \theta_1 = 0 \quad (3.6)$$

$$\frac{d^2 C_1}{dy^2} + SSc \frac{dC_1}{dy} - \gamma C_1 = -\frac{ScSo}{N} \frac{\partial^2 \theta_1}{\partial y^2} \quad (3.7)$$

The second order equations are

$$\frac{d^2 u_2}{dy^2} + S \frac{du_2}{dy} = -G(\theta_1 + NC_1) + (D^{-1} + M^2)u_2 - Au_1^2 \quad (3.8)$$

$$\frac{d^2 \theta_2}{dy^2} + SP \frac{d\theta_2}{dy} - \alpha P \theta_2 = 0 \quad (3.9)$$

$$\frac{d^2 C_2}{dy^2} + SSc \frac{dC_2}{dy} - \gamma C_2 = -\frac{ScSo}{N} \frac{\partial^2 \theta_2}{\partial y^2} \quad (3.10)$$

$$\gamma = KSc$$

The corresponding boundary conditions are

$$\begin{aligned} u_0(\pm 1) = 0, \theta_0(-1) = 0, C_0(-1) = 0 \\ \theta_0(+1) = 1, C_0(+1) = 1 \end{aligned} \quad (3.11a)$$

$$u_1(\pm 1) = 0, \theta_1(\pm 1) = 0, C_1(\pm 1) = 0 \quad (3.11b)$$

$$u_2(\pm 1) = 0, \theta_2(\pm 1) = 0, C_2(\pm 1) = 0 \quad (3.11c)$$

4. SOLUTION OF THE PROBLEM

Solving the equations (3.2)-(3.10) subject to the boundary conditions (3, 11a, b, c) we obtain

$$u_0 = a_2(\exp(-sy) - \text{Cosh}(s y))$$

$$u_1 = a_{19} + a_{20} \exp(-s y) + \phi_1(y)$$

$$\phi_1(y) = a_{11}y - a_{12}y^2 - a_{13}y \exp(-s y) - a_{14} \exp(-m_1 y) - (a_{15} + a_{16}) \exp(-m_2 y) - a_{17} \exp(-m_3 y) - a_{18} \exp(-m_4 y)$$

$$u_2 = a_{25} + a_{26} \exp(-s y) + \phi_2(y)$$

$$\phi_2(y) = a_{58}y + a_{59} + a_{60}y^2 + a_{49}y^3 + \frac{1}{2s^2} \exp(-2sy) + \frac{1}{6s^2} \exp(2sy) + a_{53} \exp(-m_1 y) + a_{54} \exp(m_2 y) + a_{55} \exp(m_3 y) + a_{56} \exp(m_4 y) + (a_{61} + a_{43}y^2 + a_{45}) \exp(-s y) + a_{57} \exp(s y)$$

$$\theta_0 = a_3 \exp(m_1 y) + a_4 \exp(m_2 y) \quad \theta_1 = 0 \quad \theta_2 = 0$$

$$C_0 = a_5 \exp(-m_3 y) + a_6 \exp(m_4 y) + a_7 \exp(-m_1 y) + a_8 \exp(m_2 y)$$

$$C_1=0, \quad C_2=0$$

5. NUSSELT NUMBER AND SHERWOOD NUMBER

The rate of heat transfer (Nusselt Number) on the boundaries $y = \pm 1$ are given by

$$(Nu)_{y=\pm 1} = \left(\frac{d\theta_0}{dy} + \delta \frac{d\theta_1}{dy} + \delta^2 \frac{d\theta_2}{dy} \right)_{y=\pm 1}$$

and the corresponding expressions are

$$(Nu)_{y=+1} = b_7 \quad (Nu)_{y=-1} = b_8$$

The rate of mass transfer (Sherwood Number) on the boundaries $y = \pm 1$ are given by

$$(Sh)_{y=\pm 1} = \left(\frac{dC_0}{dy} + \delta \frac{dC_1}{dy} + \delta^2 \frac{dC_2}{dy} \right)_{y=\pm 1}$$

and the corresponding expressions are

$$(Sh)_{y=+1} = b_9 \quad (Sh)_{y=-1} = b_{10}$$

For $S_0=0$ the results are in good agreement with sudha [10]

6. DISCUSSION OF THE NUMERICAL RESULTS

In this analysis we investigate the sores effect on the convective heat and mass transfer of a viscous electrically conducting, chemically reacting fluid in vertical channel with uniform suction. We consider three different cases $k>0$, $k=0$ and $k<0$, where k is the chemical reaction parameter. $k>0$ represents destructive chemical reaction, $k=0$ represents no chemical reaction and $k<0$ is for generative chemical reaction.

The velocity u is represented in figs.1-7 for different values of the governing parameters S_0, N_1, α and k . $u>0$ is the actual flow and $u<0$ is the reversal flow. It is found that the velocity profiles rises from its value zero on the boundary $y= -1$ attains maximum at $y=0.8$ and then falls to zero on $y=1$. The axial velocity enhances with increase in $G \leq 2 \times 10^3$ and reduces with higher $G \geq 3 \times 10^3$. It reduces with increase in the strength of the heat generating source (fig.1). From

fig-3 we notice that when the molecular buoyancy force dominates over the thermal buoyancy force the axial velocity u experiences a depreciation in the flow region when the buoyancy forces act in the same direction and for the forces acting in different directions we notice an enhancement in u in the entire flow region. Also an increase in the radiation parameter N_1 leads to depreciation in u in the entire flow region. Fig. 4 represents the behavior of u with reference to the suction parameter S . We find that $u < 0$ for $S = 1.3$ thereby indicating reversal flow in the entire region. Also u enhances with increase in $S \leq 0.5$ and depreciates with higher $S \geq 1.3$. It is found that the velocity enhances during the generative reaction ($k \leq 1.2$) and reduces with $k \geq 2$ while in the destructive reaction. Also we find a reversal flow for $k = 1.2$. Fig 6 represents the variation of u with Sc & S_0 . It is found that lesser the molecules diffusivity larger u in the flow region and for further lowering of the diffusivity smaller u in the region for $S_c \leq 2.01$ we notice a reversal flow in the region ($-0.4 \leq y \leq 0.8$). The variation of u with sorlet parameter S_0 shows that an increase in S_0 leads to a reduction in u in the left half and enhances in the right half of the region while an increase in $|S_0| (< 0)$ enhances u in the entire region.

The non-dimensional temperature (θ) is shown in figs 8-15. The temperature is found to be positive for all variations. The non-dimensional temperature enhances with increase in G and $\alpha \leq 4$ and experience a depreciation with higher $\alpha \geq 6$ (fig-8). From fig-9, we find that higher the Lorentz force larger the temperature θ . The variation of θ with buoyancy ratio N shows that when molecular buoyancy force dominates over the thermal buoyancy force the temperature experience an enhancement when the buoyancy forces act in the same direction while for the forces acting in opposite directions it reduces in the flow region (fig-10). An increase in the radiation parameter N_1 reduces θ everywhere in the flow region (Fig-11). From fig-12 we notice that an increase in the suction parameter leads to an increment in the temperature in the region $-0.8 \leq y \leq 0.8$ and is almost linear in the neighborhood of $y = 1$. The variation of θ with Schmidt number Sc shows that lesser the molecular diffusivity smaller the temperature in the flow region. The variation of θ with S_0 reveals that θ enhances with increase $S_c \geq 0$ and depreciates with $|S_0| (\geq 0)$ (Fig-14). Fig-15 represents, θ with chemical reaction parameter k . It is found that in the case of generative reaction ($k \leq 1.2$) the temperature depreciates in the left half and enhances in the right half and for higher $k > 2$ it depreciates with $k = 2$, while in the case of destructive reaction, we notice an enhancement in the temperature (Fig-15)

The concentration distribution (C) is shown in figs.16-24. We follow the convention that the concentration is positive and negative according as the actual concentration is greater or lesser than the ambient concentration. The concentration gradually rises from value to attain its prescribed value $y = 1$. The variation of C with Grashoff number G shows that the concentration experience a marginal increment with increase in the entire flow region. With respect to heat source parameter α we notice that for $\alpha \leq 4$, C is positive and is negative for higher $\alpha \geq 6$. The actual concentration enhances with α in the entire flow region (Fig-17). From fig-18 we observe that higher the Lorentz force smaller the actual concentration in the flow region (Fig-18). The variation of C with N shows that C is positive for $N > 0$ and negative in the left half for $N < 0$. When the molecular buoyancy force dominates over the thermal buoyancy force, the actual concentration experiences a depreciation in the entire flow region, while for the forces acting in opposite direction the actual concentration increases in the flow region (Fig-19). An increase in N_1 enhances the actual concentration in the flow region (Fig-20). Also an increase in the suction parameter S leads to an increment in the concentration (Fig-21). A variation of C with Schmidt number Sc reveals that the concentration is positive for all values of Sc except for $Sc = 0.6$ where it is negative. It is found that the concentration enhances with $Sc \leq 0.6$ and depreciates with higher $Sc \geq 0.3$ (Fig-22). From fig-23 we find that an increase in S_0 results in an enhancements in concentration while in increase in $|S_0| < 0$ leads to a depreciation in the concentration. The variation of C with chemical reaction parameter k in the case of generating reaction, C is negative in the vicinity of $y = -1$ and positive everywhere while in the case of destructive reaction it is negative in the region $-0.8 \leq y \leq -0.6$. It is found that the concentration experiences an enhancement with $k \leq 1.2$ and depreciates with higher $k \geq 2$ while an increase in $|k| (< 0)$ the concentration depreciates in the entire flow region.

The Nusselt number which represents the rate of heat transfer at $y = \pm 1$ is shown in table 1-6. It is found that the rate of heat transfer experiences an enhancement in magnitude with increase in $|G| (< > 0)$. An increase in the suction parameter S , depreciates $|Nu|$ at $y = 1$ and enhances it at $y = -1$ (tables 3 & 6). The variation of Nu with heat source parameter α indicates that $|Nu|$ experiences an enhancement with α at $y = 1$ and depreciates at $y = -1$. The variation of Nu with Sc reveals that lesser the molecular diffusivity larger $|Nu|$ and for further lowering of the molecular diffusivity smaller $|Nu|$ and for still lowering of the diffusivity larger $|Nu|$ at $y = 1$. while at $y = -1$ larger $|N|$. With respect to variation in S_0 , we notice that $|Nu|$ depreciates with increase in $|S_0| > 0$ and enhances with $|S_0| (< 0)$ (tables 2 & 5). An increase in the radiation parameter N_1 enhances the rate of heat transfer at $y = 1$ and at $y = -1$ it enhances with $N_1 \leq 1$ and depreciates with $N_1 \geq 1.5$. The variation of Nu with chemical reaction parameter k shows that the rate of heat transfer enhances in the generating reaction and depreciates in the destructive reaction (tables 1 & 4).

The Sherwood number (Sh) which represents the rate of mass transfer at $y = \pm 1$ is shown in table 7-12 for different values of the governing parameter. It is found that the rate of mass transfer enhances with increasing $G > 0$ at both the walls while an increase in $|G| (< > 0)$ enhance $|Sh|$ at $y = 1$ and depreciates at $y = -1$. Also an increase in the suction parameter S leads to a reduction $|Sh|$. (tables 9 & 12). The variation of Sh with Sc shows that lesser the molecular

diffusivity smaller $|Sh|$ and for further lowering of diffusivity larger $|Sh|$ at $y=1$ while larger the rate of mass transfer at $y= -1$. An increase in the solet parameter $S_0 > 0$ enhances the Sherwood number at $y=1$ and depreciates at $y= -1$, while an increase in $|S_0| (< 0)$ enhances it at $y= \pm 1$ (tables 8 & 11). From tables 7 & 10, we notice that $|Sh|$ decreases in the generating reaction and enhances in the destructive reaction, while a reversed effect is observed at $y= -1$.

7. REFERENCES

- [1] Angirasaa,D,Peterson,G.P and Pop,I :Combined heat and mass transfer by natural convection with opposing buoyancy effects in a fluid saturated porous medium ,Int.J.HeatMassTransfer(1997),V.40,pp.2755-2773
- [2] Bejan,A and Khair,K.R: Heat and Mass transfer by natural convection in a porous medium,Int.J.Heat Mass transfer, (1985)V.28,pp.908-918
- [3] Lai,F.C :Cpupled heat and mass transfer by mixed convection from a vertical plate in a saturated porous medium.,Int.Commn.heat mass transfer(1971),,V.18,pp.93-106
- [4] Lai,F.C and Kulacki,F.A : Coupled heat and mass transfer by natural convection from vertical surfaces in porous medium.,Int.J.Heat Mass Transfer, (1991),V.34,pp.1189- 1194
- [5] Murthy,P.V.S.N and Singh,P:Heat and Mass transfer by natural convection in a Non-Darcy porous medium,Acta Mech, (1990),V.26,pp.567
- [6] Nelson,D.J and Wood,B.D: Combined heat and mass transfer by natural convection between vertical plates with uniform flux boundary conditions,Heat transfer(1986),V.4,pp.1587-1952
- [7] Nelson,D.J and Wood,B.D: Combined heat and mass transfer by natural convection between vertical plates ,Int.J.,Heat Mass transfer, (1989),V.82,pp.1789-1792
- [8] Prasad,V,Kulacku,F.A and Keyhani,M:Natural convection in a porous medium,J.Fluid Mech. (1985),V.150,pp.89-119
- [9] Raptis, A.A and Perdikis, C Radiation and free convection flow past a moving plate, Appl. Mech. Eng, (1999), Vol.4, pp 817-821.
- [10] Sudha Mathew: Hydro magnetic mixed convective heat and mass transfer through a porous medium in a vertical channel with thermo-diffusion effect. Ph.D thesis, S,K. University, Anantapur, India(2009).
- [11] Trevison ,D.V and Bejan,A :Combined heat and mass transfer by natural convection in vertical enclosure, Trans. ASME(1987),V.109,pp.104-111
- [12] Wei-Mon Yan:Combined buoyancy effects of thermal and mass diffusion on laminar forced convection in horizontal rectangular ducts,Int,J,Heat Mass transfer, (1996),V.39,pp.1479-1488

Figures:

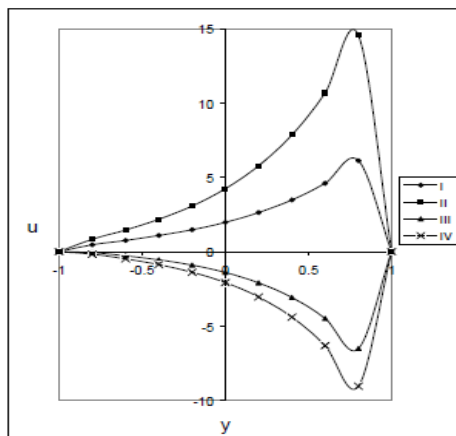


Fig.3 Variation of U with N
 $M=2, G=10^3, K=2$

I	II	III	IV	
N	1	2	-0.5	-0.8

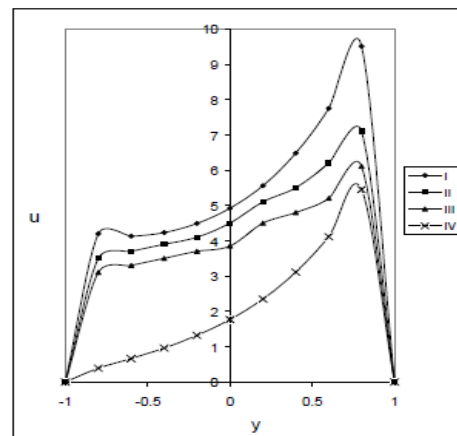


Fig.4 Variation of U with N1
 $M=2, G=10^3, K=2$

I	II	III	IV	
N ₁	0	5	10	100

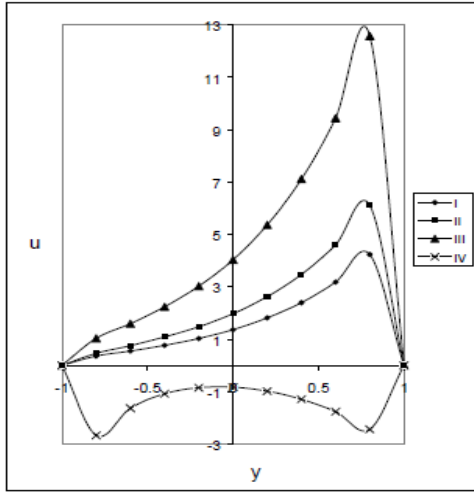


Fig.5 Variation of u with S
 $M=2, G=10^3, K=2$

	I	II	III	IV
S	0.1	0.3	0.5	1.3

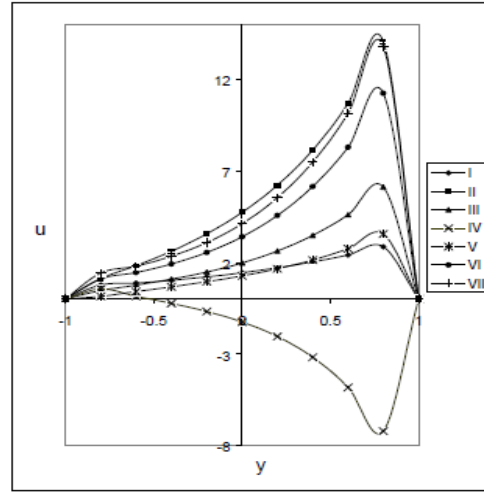


Fig.6 U with Sc & S_0
 $M=2, G=10^3, K=2$

	I	II	III	IV	V	VI	VII
Sc	0.24	0.6	1.3	2.01	1.3	1.3	1.3
S_0	0.5	0.5	0.5	0.5	1	-0.5	-1

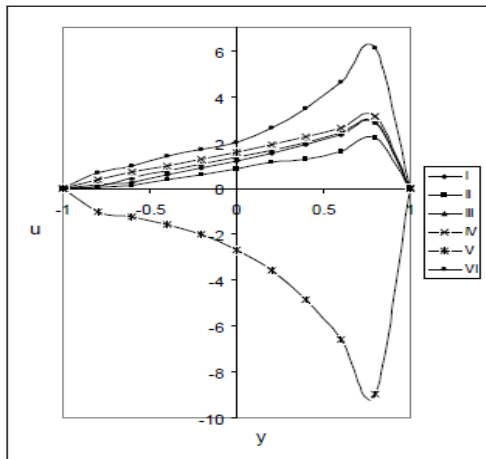


Fig.7 Variation of U with K
 $M=2, G=10^3, N=1$

	I	II	III	IV	V	VI
K	-0.2	-0.02	0	0.2	1.2	2

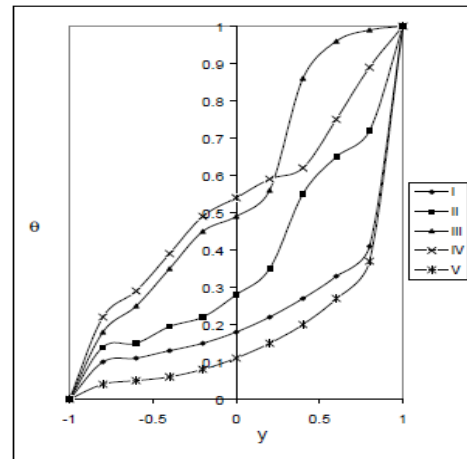


Fig.8 Variation of θ with G & α

	I	II	III	IV	V
G	1×10^3	3×10^3	5×10^3	3×10^3	3×10^3
α	2	2	2	4	6

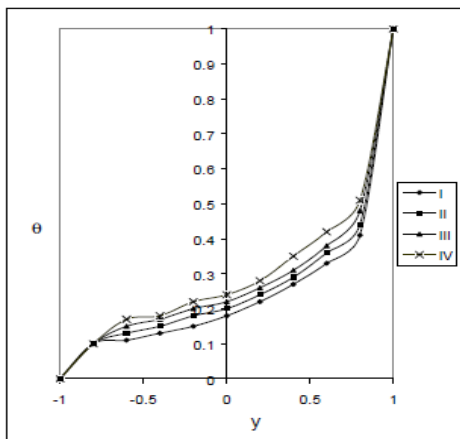


Fig.9 Variation of θ with M
 $K=2, G=10^3, N=1$

	I	II	III	IV
M	0	2	3	4

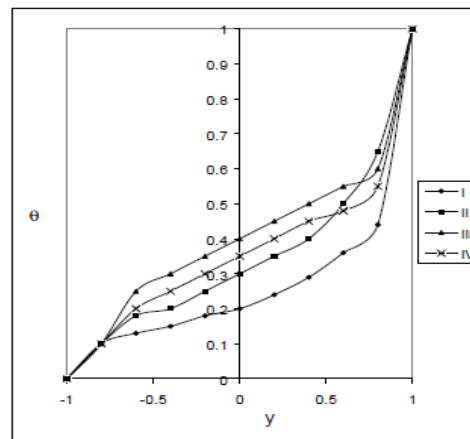


Fig.10 Variation of θ with N
 $M=2, G=10^3, K=2$

	I	II	III	IV
N	1	2	-0.5	-0.8

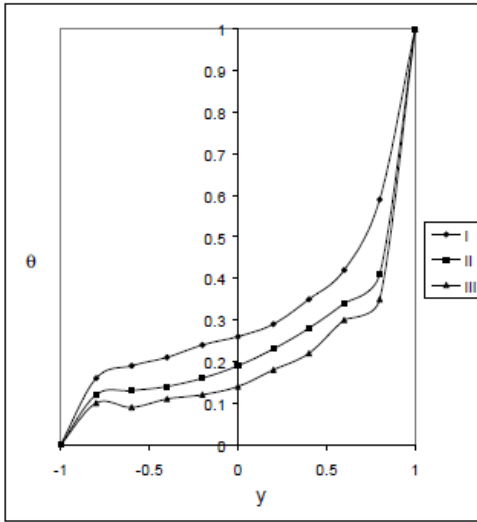


Fig.11 Variation of θ with N_1
 $M=2, G=10^3, N=1$

	I	II	III
N_1	0	5	10

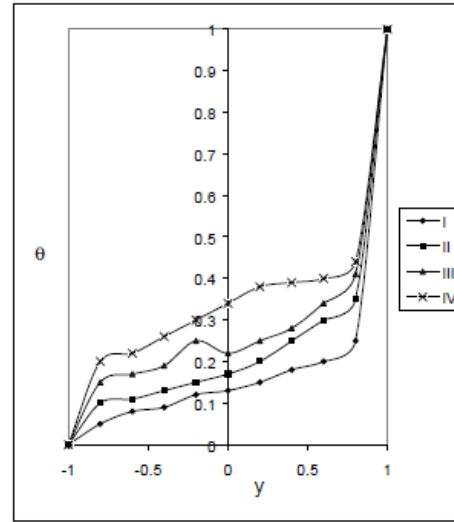


Fig.12 Variation of θ with S
 $M=2, G=10^3, N=1$

	I	II	III	IV
S	0.1	0.3	0.5	1.3

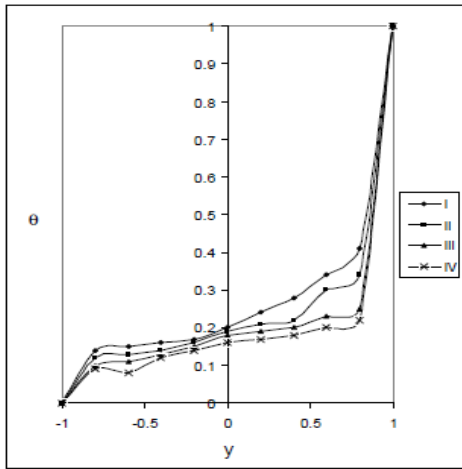


Fig.13 Variation of θ with Sc
 $M=2, G=10^3, N=1$

	I	II	III	IV
Sc	0.24	0.6	1.3	2.01

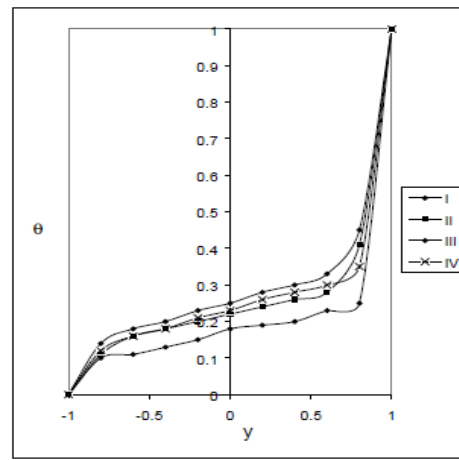


Fig.14 Variation of θ with S_0
 $M=2, G=10^3, N=1$

	I	II	III	IV
S_0	0.5	1	-0.5	-1

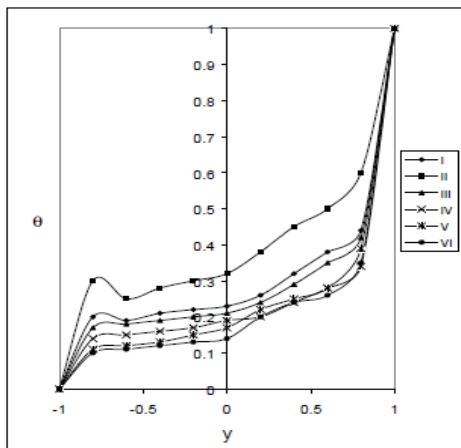


Fig.15 Variation of θ with K
 $M=2, G=10^3, N=1$

	I	II	III	IV	V	VI
K	-0.2	-0.02	0	0.2	1.2	2

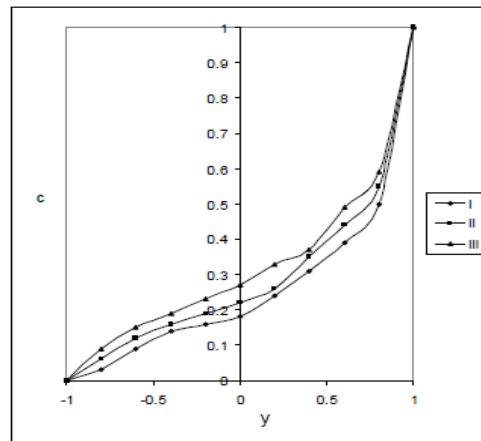


Fig.16 Variation of C with G
 $M=2, K=2, N=1$

	I	II	III
G	1×10^3	3×10^3	5×10^3

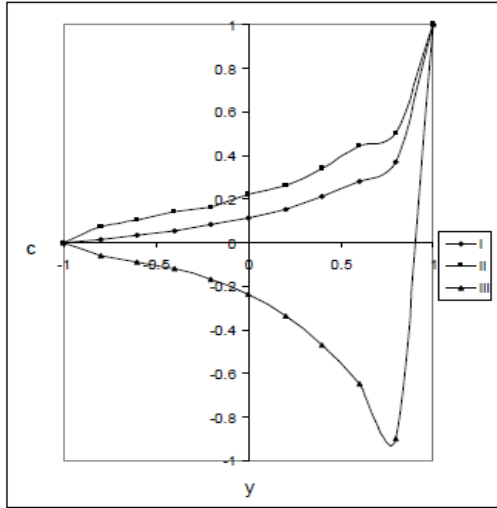


Fig.17 Variation of C with α
 $M=2, G=10^3, N=1$

I	II	III	
α	2	4	6

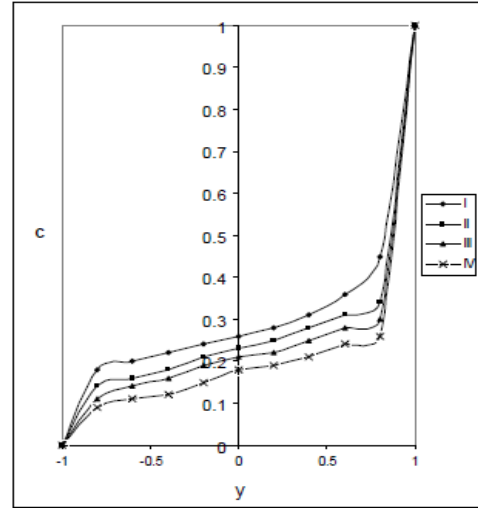


Fig.18 Variation of C with M
 $K=2, G=10^3, N=1$

I	II	III	IV	
M	0	2	3	4

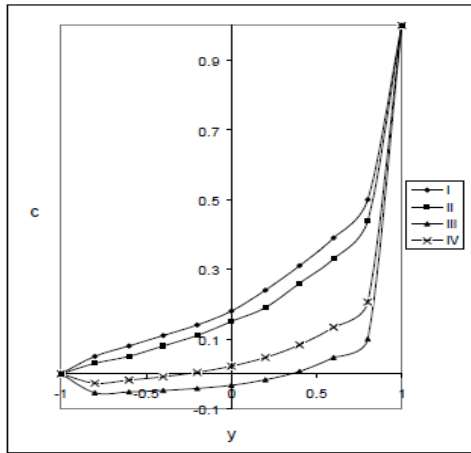


Fig.19 Variation of C with N
 $M=2, G=10^3, K=2$

I	II	III	IV	
N	1	2	-0.5	-0.8

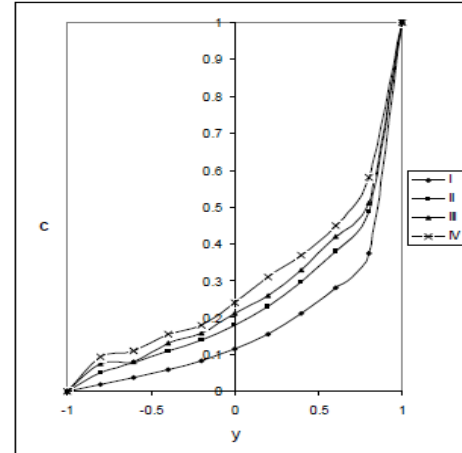


Fig.20 Variation of C with N_1
 $M=2, G=10^3, N=1$

I	II	III	IV	
N_1	0	5	10	100

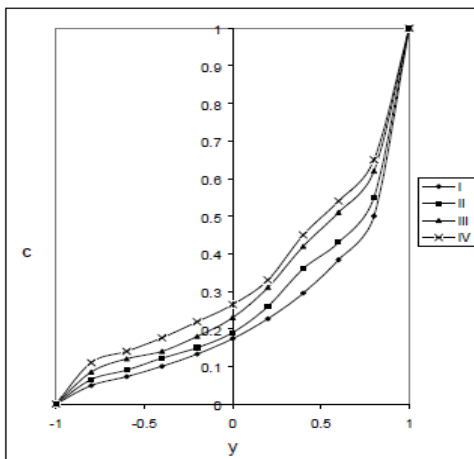


Fig.21 Variation of C with S
 $M=2, G=10^3, N=1$

I	II	III	IV	
S	0.1	0.3	0.5	1.3

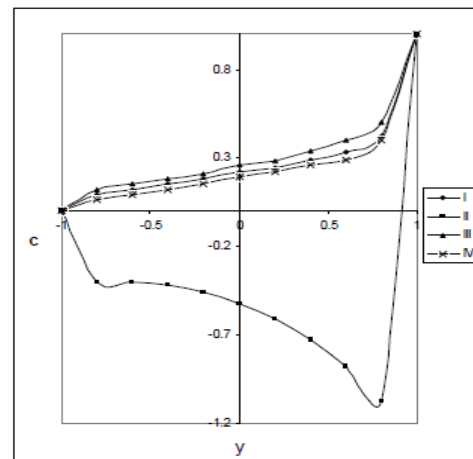


Fig.22 Variation of C with Sc
 $M=2, G=10^3, N=1$

I	II	III	IV	
Sc	0.24	0.26	1.3	2.01

Tables:

Table.1
Nusselt Number (Nu)at y = 1
G=10³, M= 2.00, N= 1.00, S_c=1.30, S_o=0.5, S=0.30

α	I	II	III	IV	V	VI	VII	VIII
2	0.29982	0.29869	0.25595	0.0987	0.0861	0.17911	0.40092	0.48163
4	0.51994	0.46133	0.45070	0.27625	0.1969	0.37414	0.57701	0.57673
6	0.56654	0.53859	0.43951	0.39905	0.2509	0.52758	0.80478	0.82536
K	2	1	0.5	-0.01	-0.02	2	2	2
N ₁	0.5	0.5	0.5	0.5	0.5	1.0	1.5	5.00

Table.2
Nusselt Number (Nu)at y=1
G=10³, M= 2.00, N= 1.00, S_c=1.30, S_o=0.5, S=0.30

α	I	II	III	IV	V	VI	VII
2	0.29982	0.32883	0.31955	0.36063	0.29618	0.30658	0.30969
4	0.41994	0.44786	0.22679	0.42560	0.41581	0.42601	0.42794
6	0.51654	0.54114	0.51676	0.56817	0.51162	0.52042	0.53937
S _c	1.30	2.01	0.24	0.60	1.30	1.30	1.30
S _o	0.5	0.5	0.5	0.5	1.0	-0.5	-1.00

Table.3
Nusselt Number (Nu)at y=1
G=10³, M= 2.00, N= 1.00, S_c=1.30, S_o=0.5, S=0.30

α	I	II	III	IV	V	VI
2	0.29982	0.31384	0.34373	0.40166	0.31617	0.28094
4	0.41994	0.42522	0.46181	0.50895	0.43506	0.40294
6	0.51654	0.51738	0.55120	0.58570	0.53069	0.50141
G	10 ³	3×10 ³	5×10 ³	10 ³	10 ³	10 ³
S	0.3	0.3	0.3	1.3	0.1	0.5

Table.4
Nusselt Number (Nu)at y=-1
G=10³, M= 2.00, N= 1.00, S_c=1.30, S_o=0.5, S=0.30

α	I	II	III	IV	V	VI	VII	VIII
2	- 0.16142	0.31538	0.28048	- 0.16726	- 0.1492	- 0.21397	- 0.11834	- -0.07365
4	- 0.10806	0.11302	- 0.03611	- 0.12598	- 0.1054	- 0.16301	- 0.10219	- 0.085807
6	- 0.05312	- 0.18289	- 0.06285	- 0.10533	- 0.0269	- 0.12580	- 0.06668	- -0.06176
K	2	1	0.5	-0.01	-0.02	2	2	2
N ₁	0.5	0.5	0.5	0.5	0.5	1.0	1.5	5.00

Table.5

Nusselt Number (Nu) at $y=-1$

$G=10^3$, $M= 2.00$, $N= 1.00$, $S_c=1.30$, $S_o=0.5$, $S=0.30$

α	I	II	III	IV	V	VI	VII
2	-0.16142	0.33710	0.05822	-0.10839	-0.14277	-0.19872	-0.21737
4	-0.10806	0.25899	-2.31503	0.66831	-0.06924	-0.18572	-0.22454
6	-0.05312	0.19333	-0.02399	0.0473	0.01375	-0.18686	-0.25373
S_c	1.30	2.01	0.24	0.60	1.30	1.30	1.30
S_o	0.5	0.5	0.5	0.5	1	-0.5	-1.00

Table.6

Nusselt Number (Nu) at $y=-1$

$G=10^3$, $M= 2.00$, $N= 1.00$, $S_c=1.30$, $S_o=0.5$, $S=0.30$

α	I	II	III	IV	V	VI
2	-0.16142	-0.41729	0.35031	0.60618	-0.10680	-0.36946
4	-0.10806	-0.29483	0.26548	0.45224	-0.07259	-0.25061
6	-0.05312	-0.17102	0.18267	0.30057	-0.03725	-0.12383
G	10^3	3×10^3	5×10^3	10^3	10^3	10^3
S	0.3	0.3	0.3	1.3	0.1	0.5

Table.7

Sherwood Number (Sh) at $y=1$

$G=10^3$, $M= 2.00$, $N= 1.00$, $S_c=1.30$, $S_o=0.5$, $S=0.30$

α	I	II	III	IV	V	VI	VII	VIII
2	0.02361	0.07967	0.38660	0.34430	0.4562	0.22573	0.4927	0.00118
4	0.11677	0.14243	-0.24939	0.21412	0.3402	0.17995	0.29760	4.62907
6	0.0493	-0.12619	0.18628	0.18628	0.2412	0.16464	2.20539	1.00983
K	2	1	0.5	-0.01	-0.02	2	2	2
N_1	0.5	0.5	0.5	0.5	0.5	1.0	1.5	5.00

Table.8

Sherwood Number (Sh) at $y=1$

$G=10^3$, $M= 2.00$, $N= 1.00$, $S_c=1.30$, $S_o=0.5$, $S=0.30$

α	I	II	III	IV	V	VI	VII
2	0.02361	0.06378	0.11776	0.07016	0.00785	0.06779	0.09622
4	0.01677	0.08725	3.51521	0.08839	0.00652	0.09204	0.15908
6	0.00693	0.10146	0.13141	0.063510	0.00340	0.12490	0.26340
S_c	1.30	2.01	0.24	0.60	1.30	1.30	1.30
S_o	0.5	0.5	0.5	0.5	1	-0.5	-1.00

Table.9

Sherwood Number (Sh) at $y=1$

$G=10^3, M= 2.00, N= 1.00, S_c=1.30, S_o=0.5, S=0.30$

α	I	II	III	IV	V	VI
2	0.02361	-0.0534	0.08233	0.11209	0.02400	0.00577
4	0.01677	-0.03038	0.11173	0.15954	0.01693	-0.00831
6	0.00693	-0.02711	0.12947	0.18197	0.01786	0.00187
G	10^3	3×10^3	5×10^3	10^3	10^3	10^3
S	0.3	0.3	0.3	1.3	0.1	0.5

Table.10

Sherwood Number (Sh) at $y=-1$

$G=10^3, M= 2.00, N= 1.00, S_c=1.30, S_o=0.5, S=0.30$

α	I	II	III	IV	V	VI	VII
2	0.66960	0.40448	-0.02557	0.23836	0.08391	0.61457	0.53126
4	0.80044	0.07105	0.61159	0.10229	0.04274	0.30307	13.48605
6	1.77601	1.56135	0.82357	0.06057	0.01896	24.33248	1.42910
K	2	1	0.5	-0.01	2	2	2
N_1	0.5	0.5	0.5	0.5	1.0	1.5	5.00

Table.11

Sherwood Number (Sh) at $y=-1$

$G=10^3, M= 2.00, N= 1.00, S_c=1.30, S_o=0.5, S=0.30$

α	I	II	III	IV	V	VI	VII
2	0.66960	0.81949	0.27469	0.47137	0.62425	0.75611	0.79690
4	0.80044	0.75733	0.14776	0.34424	0.48429	0.82190	0.92170
6	1.77601	0.66765	0.36692	1.94325	0.24356	0.79690	1.13196
S_c	1.30	2.01	0.24	0.60	1.30	1.30	1.30
S_o	0.5	0.5	0.5	0.5	1	-0.5	-1.00

Table.12

Sherwood Number (Sh) at $y=-1$

$G=10^3, M= 2.00, N= 1.00, S_c=1.30, S_o=0.5, S=0.30$

α	I	II	III	IV	V	VI
2	0.66960	0.66771	0.68157	0.69166	0.72730	0.61404
4	0.60044	0.59676	0.62109	0.63805	0.66080	0.54073
6	0.47601	0.46802	0.50718	0.53038	0.55362	0.38918
G	10^3	3×10^3	5×10^3	10^3	10^3	10^3
S	0.3	0.3	0.3	1.3	0.1	0.5
